Presented at the 25th European PV Solar Energy Conference and Exhibition, 6-10 September 2010, Valencia, Spain

CONDUCTIVITY MOBILITY AND HALL MOBILITY IN COMPENSATED MULTICRYSTALLINE SILICON

F. Schindler[1], J. Geilker[1], W. Kwapil[1], J. Giesecke[1], M.C. Schubert[1], W. Warta[1]
[1] Fraunhofer Institute for Solar Energy Systems (ISE)
Heidenhofstraße 2, 79110 Freiburg, Germany
Phone: +49 761 4588 5560; Fax: +49 761 4588 9250
Email: Florian.Schindler@ise.fraunhofer.de

ABSTRACT: The knowledge of the majority carrier mobility in silicon as a function of dopant density is of utmost importance for a correct quantitative evaluation of a variety of lifetime measurements. However, only for monocrystalline silicon doped with either boron (concentration N_A) or phosphorus (concentration N_D), sufficient reliable experimental data exists as well as good models. In the presence of both dopants, in so called compensated silicon, a reduced mobility is expected. It seems that the model of Klaassen provides acceptable values for the mobility in lowly compensated monocrystalline silicon as a function of $N_A + N_D$ [1]. For more strongly compensated monocrystalline silicon and for multicrystalline silicon, it is not sure if this model is still applicable. In this contribution, the conductivity mobility of majority carrier holes as well as the Hall mobility in compensated and non-compensated multicrystalline (mc) p-type silicon is investigated and compared with the established mobility models as well as with the data from monocrystalline silicon.
Keywords: Multicrystalline Silicon, Mobility, Compensation

1 INTRODUCTION

Besides its direct relation to the solar cell performance, carrier mobility plays an important role in various lifetime techniques. In a QSSPC measurement, for instance, a difference in conductivity $\Delta\sigma$ is measured, which is proportional to the injection level Δn as well as to the sum of minority carrier mobility μ_{min} and majority carrier mobility μ_{maj}: $\Delta\sigma \sim \Delta n \cdot (\mu_{maj} + \mu_{min})$. The lifetime itself is proportional to Δn. So if the sum of the mobilities is overestimated by a certain factor, the measured lifetime is underestimated by the same factor. A contrary effect of a false mobility value can be seen in a PL lifetime measurement, if the net doping p_0 is determined via a resistivity measurement and the majority carrier mobility μ_{maj}: $p_0 = (\rho \cdot q \cdot \mu_{maj})^{-1}$. In this method, the measured PL signal Φ for low injection levels is proportional to Δn and p_0: $\Phi \sim \Delta n \cdot p_0$. As one can see, an overestimation of the mobility leads to an underestimation of the net doping p_0, which itself again leads to an overestimation of Δn and therefore to an overestimation of lifetime. This demonstrates that the knowledge of an exact mobility value is of great interest.

Although the knowledge of the minority carrier mobility is not of less interest, this paper is restricted to investigations on the majority carrier mobility. An approach to measure the minority carrier mobility via photoconductance decay [2] is made by F.E. Rougieux et al. in compensated silicon [3].

Several material characteristics can influence the carrier mobility. In mc silicon, the influence of both different levels of compensation as well as different densities of crystal defects like grain boundaries and dislocations on the carrier mobility is investigated.

2 EXPERIMENTAL METHODS

There are different ways to determine the majority carrier mobility in silicon wafers. The easiest way to measure the mobility directly is a Hall measurement [4]. This method uses the Hall Effect to determine the Hall coefficient R_H, which together with a resistivity measurement leads to the Hall mobility. From the measured Hall mobility μ_H the conductivity mobility μ_C can be deduced if the Hall scattering factor r is known, which links both mobilities via $\mu_H = r \cdot \mu_C$. Although several theoretical models for the description of the Hall factor as a function of dopant density exist [5, 6], there are discrepancies with measured data. The determination of this Hall factor for different levels of compensation in mc silicon is one aim of this investigation. To get the value of the Hall factor, the conductivity mobility has to be measured independently by other methods. Therefore we applied the approach explained in another contribution by J. Geilker at the same conference [7]. The combination of a resistivity (ρ) measurement and the measurement of the net doping p_0 ($p_0 = N_A - N_D$ in p-type silicon; neglecting incomplete ionization) leads to the conductivity mobility via the relation $1/\rho = q \cdot p_0 \cdot \mu_C$, where q is the elementary charge. Electrochemical capacitance-voltage (ECV) measurements provide the net doping p_0. Afterwards the Hall factor is determined by a comparison of the conductivity mobility and the measured Hall mobility.

	mc46	**umg30**	**umg85**
type	p	p compensated	p compensated
ρ [Ωcm]	0.90	0.77	0.84 - 1.06
N_A [10^{16} cm^{-3}]	1.69	4.53	6.08
p_0 [10^{16} cm^{-3}]	1.69	2.65	(2.34 - 2.91)
N_D [10^{16} cm^{-3}]	0	1.88	(3.74 - 3.17)

Table I: Sample characteristics

For the investigations, three samples were chosen (Table I): One p-type mc silicon wafer from the middle of an uncompensated block (at a position of 46% of the block height, measured from the bottom), in the following signified with “mc46”, one p-type mc silicon wafer from the middle of a compensated umg (upgraded

metallurgical grade)-Si block (at a position of 30% of the block height), in the following "umg30", and one p-type mc silicon wafer from the top of the same umg-Si block (at a position of 85% of the block height), "umg85".

To investigate the influence of grain boundaries and dislocations on the mobility, the 1 x 1 cm^2 Hall samples were selected from different areas: Areas with a low density of grain boundaries and dislocations and from regions with a higher density of grain boundaries and dislocations. The Hall samples were chosen with the help of optical pictures of the wafers and photoluminescence images (PLI), where recombination active grain boundaries and dislocations are visible. Within the ten Hall samples per wafer, several types of grain structures were present: Samples without any visible grain structure, where the grain size was larger than 1 x 1 cm^2 (quasi monocrystalline samples), samples with low density of grain boundaries and dislocation clusters and such with both a high density of grain boundaries and dislocations. To determine the resistivity, four-point-probe measurements were realized in all these areas as well as manual thickness measurements. The net doping p_0 was measured via ECV measurements (with a correction factor accounting for the crater area [8]), the acceptor concentration N_A in the compensated wafers via the iron-acceptor pairing method [9, 7]. The donor concentration N_D was determined as difference of the acceptor concentration and the net doping $N_A - p_0$.

After laser-cutting of the samples and contacting the four corners, Hall mobility measurements could be realized.

3 RESULTS

3.1 Resistivity measurements

The resistivities measured by the four-point-probe technique on the samples of the uncompensated wafer (mc46) and the umg wafer from the block middle (umg30) are relatively homogeneous over the whole wafer area, independent from grain boundaries and dislocations. Therefore the resistivity could be averaged on these two wafers (Table II). The result for the umg wafer from the block top, umg85, was slightly different. Here the resistivity fluctuated significantly over the wafer area (Table III). As a systematic dependence on certain grain structures or dislocations was not observed, this fluctuation was attributed to fluctuations in the net doping, which occur in the top region of umg blocks: While in the centre of the block, during crystallisation dopants are distributed homogeneously over the wafer, in the top region the inhomogeneous crystallisation front leads to differences in the net doping over the wafer which influences the resistivity. The ECV measurements of p_0 confirmed this assumption.

	mc46	**umg30**
ρ [Ωcm]	0.90±0.02	0.77±0.02
μ_H [cm^2/Vs]	301±4	238±3

Table II: Resistivity and Hall mobility of the two homogeneous samples **mc46** and **umg30**

3.2 Measuring p_0 and N_A

The ECV measurements were realized on one representative spot on each wafer. As the resistivity was homogeneous on mc46 and umg30, no fluctuation in the net doping was expected for these samples. After crater area correction we got $p_0 = 1.69 \times 10^{16}$ cm^{-3} for mc46 and $p_0 = 2.65 \times 10^{16}$ cm^{-3} for umg30. For umg85 the ECV measurements were realized in two different spots, leading to different values in the net doping. One measurement showed a constant profile of net doping over the etched depth, whereas the other measurement showed fluctuations in net doping with the etched depth. The maximum net doping was $p_0 = 2.91 \cdot 10^{16}$ cm^{-3} and the minimum net doping was $p_0 = 2.34 \cdot 10^{16}$ cm^{-3}. N_A was measured by the iron-acceptor pairing method realized with a QSSPC measurement of the lifetime decay in the dark. For results see Table I. Afterwards N_D was determined in the compensated samples via $N_D = N_A - p_0$.

3.3 Determination of the Hall mobility μ_H

In order to determinate the influence of grain boundaries and dislocations on the mobility, Hall measurements were realized on all ten Hall samples per wafer. Interestingly, the Hall mobilities do not vary significantly in one wafer, neither in the non-compensated nor in the compensated ones. The average values of mc46 and umg30 are listed in Table II. Even in umg85, where we observed fluctuations in resistivity as well as in net doping concentration, a significant variation in the Hall mobility is not measured (Table III). This leads to the conclusion, that the fluctuations in resistivity are based on fluctuations in the net doping concentration p_0, which equals the difference of the dopant concentrations N_A - N_D, whereas μ_H is determined by the total concentration of dopants $N_A + N_D$. Therefore a little variation in the doping concentrations N_A and N_D may substantially affect their difference, while leaving their sum almost unaffected. Consequently, strong variations in net doping p_0 but little variation in Hall mobility are observed.

Furthermore, in this material a significant influence of grain boundaries or dislocations on the Hall mobility cannot be observed.

Hall sample	ρ [Ωcm]	μ_H [cm^2/Vs]
umg85-01	1.03	219
umg85-02	1.02	-
umg85-03	1.00	219
umg85-04	0.97	221
umg85-05	1.02	214
umg85-06	0.98	220
umg85-07	1.06	213
umg85-08	0.97	223
umg85-09	0.95	222
umg85-10	0.84	217
average	-	219±3

Table III: Resistivity and Hall mobility of wafer **umg85**

3.4 Determination of the majority hole conductivity mobility μ_C

With the data from resistivity and ECV measurements, the majority hole conductivity mobility

can be determined via $\mu_C = (q \cdot p_0 \cdot \rho)^{-1}$, where q is the elementary charge (Table IV). On each ECV sample the resistivity was determined via four-point-probe measurements. For the homogeneous wafers mc46 and umg30 this leads to majority hole mobilities of $\mu_C = (402\pm21)$ cm^2/Vs (mc46) and $\mu_C = (310\pm17)$ cm^2/Vs (umg30). For umg85 the homogeneous ECV profile (3.2) was used in combination with a resistivity measurement on the same sample. This leads to a majority hole mobility of $\mu_C = (261\pm13)$ cm^2/Vs, which should be constant over the whole wafer, as the Hall measurements illustrated.

	mc46	**umg30**	**umg85**
ρ [Ωcm]	0.92	0.76	1.025
p_0 [10^{16} cm^{-3}]	1.69	2.65	2.34
μ_C [cm^2/Vs]	402±21	310±17	261±13

Table IV: Conductivity mobilities

3.5 Hall factor

Due to scattering mechanisms in the presence of a magnetic field, being for example the case in a Hall measurement setup, the Hall mobility does not equal the conductivity mobility, which is the needed parameter for device simulation. The ratio of Hall mobility and conductivity mobility is the so called Hall factor $r = \mu_H / \mu_C$. Based on the averaged Hall mobilities and the conductivity mobilities, we obtain the Hall factors listed in Table V.

	mc46	**umg30**	**umg85**
μ_{Hall} [cm^2/Vs]	301	238	219
μ_C [cm^2/Vs]	402	310	261
r	0.75±0.04	0.77±0.04	0.84±0.04

Table V: Hall factors

3.6 Comparison with models

Figure 1 shows a plot of all measured mobilities and mobility models for comparison. Note that conductivity and Hall mobilities are plotted in the same graph. The shift in the absolute level between Hall mobilities and conductivity mobilities is attributed to the Hall factor. For not compensated material, the model of Caughey and Thomas [10], which is implemented in the PC1D software and takes into account only one dopant species as scattering centre, is applied. In compensated material both dopants, acceptors as well as donors, act as scattering centres and have to be considered. Therefore we compare the mobilities in the compensated wafers with the model of Klaassen [11], which takes into account the main contributions to scattering: lattice scattering, donor and acceptor scattering as well as electron-hole scattering. Also the screening of impurities by charge carriers and the temperature dependence are included. All mobilities are simulated at a temperature of 300 K. The closed symbols in Figure 1 represent the measured conductivity mobilities, the open symbols the Hall mobilities. All mobilities are plotted versus the acceptor concentration N_A. The conductivity mobility of mc46 (red closed square) shows good agreement with the mobility of Caughey-Thomas (cyan line) as well as with

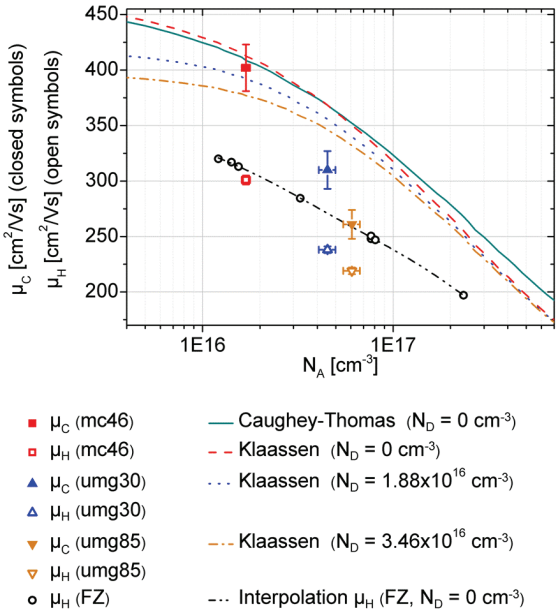

Figure 1: Measured mobilities compared with mobility models

Klaassen's mobility for $N_D = 0$ cm^{-3} (red dashed line), as expected for not compensated material. For comparison of the Hall mobilities, the black dashed-dotted line shows an interpolation of measured Hall mobilities in FZ material. The Hall mobility of mc46 (red open square) is slightly lower than expected from the FZ material, but still in reasonably good agreement. A different result is obtained for the compensated material: The conductivity mobility in umg30 (blue closed triangle pointing upwards) and in umg85 (orange closed triangle pointing downwards) is significantly lower than predicted by Klaassen (blue dotted line for umg30 and orange dashed dotted line for umg85), although in Klaassen's model both dopant species are taken into account as scattering centres (Table VI). The higher the compensation, the higher is the discrepancy between measured mobility and model.

	mc46	**umg30**	**umg85**
μ_C [cm^2/Vs]	402	310	261
$\mu_{Klaassen}$ [cm^2/Vs]	413	355	332
$\mu_C / \mu_{Klaassen}$	0.97	0.87	0.79

Table VI: Comparison of conductivity mobilities in mc and umg silicon with Klaassen's model.

	mc46	**umg30**	**umg85**
μ_{Hall} [cm^2/Vs]	301	238	219
$\mu_{Hall, FZ}$ [cm^2/Vs]	310	256	240
$\mu_{Hall} / \mu_{Hall, FZ}$	0.97	0.93	0.91

Table VII: Comparison of Hall mobilities in mc and umg silicon with those in FZ silicon at the same sum of dopant concentrations $N_A + N_D$

A confirmation that the mobility in compensated mc silicon is lower than predicted is also delivered by the measured Hall mobilities. Figure 2 shows a comparison of the Hall mobilities investigated here with the Hall

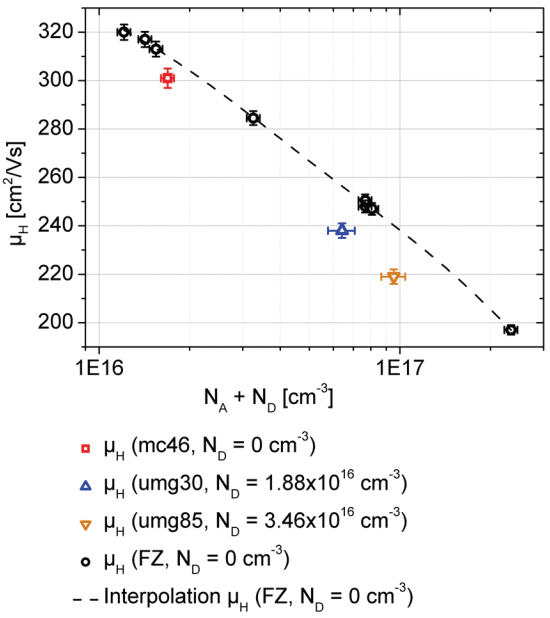

Figure 2: Hall mobilities plotted versus ($N_A + N_D$)

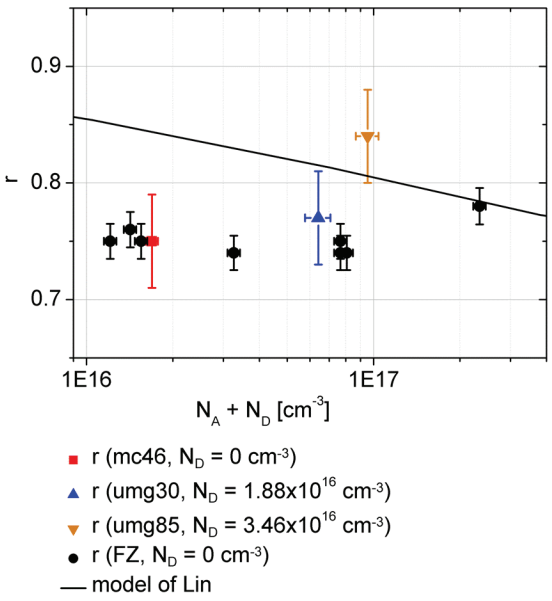

Figure 3: Measured Hall factors compared with Lin's model.

mobilities measured in FZ material. For comparative reasons, all Hall mobilities are plotted versus ($N_A + N_D$) in Figure 2. The ratio of the Hall mobilities of the multicrystalline samples and the Hall mobilities of the FZ references decreases with increasing dopant concentrations ($N_A + N_D$) (Table VII), but not as strong as the discrepancy between the measured conductivity mobilities and Klaassen's model.

This fact can also be seen regarding the measured Hall factors (Figure 3, Table V). The strong decrease in conductivity mobility and the relatively slight decrease in the Hall mobility results in an increasing Hall factor with increasing dopant concentration ($N_A + N_D$). This contradicts Lin's model [5], who predicts a decreasing Hall factor with increasing acceptor concentration. However, this result has to be regarded carefully, because Lin does not take into account the presence of both dopant species. Considering the relatively large error, it has to be proven in future work if the Hall factor really increases with increasing compensation. The Hall factors measured for mc46 and umg30 are in good agreement with those measured in FZ material of similar dopant concentration as well as with those predicted by Szmulowicz [6], who calculates a Hall factor of about $r = 0.75$ for dopant concentrations of about 10^{16} cm^{-3}.

4 DISCUSSION

As we investigated the mobility in compensated multicrystalline silicon, a comparison with compensated monocrystalline silicon is useful. On that material contradictory results are reported: While the investigations by J. Geilker [7] as well as those by F.E. Rougieux [3] show a relatively good agreement with Klaassen's model, J. Libal [12] measures a strong reduction in Hall mobility, which is in contradiction with simulations. According to our investigations, a decreasing Hall factor with increasing dopant concentration, as it was proposed in [12], cannot explain the strong decrease in the Hall mobility.

The comparison with compensated monocrystalline silicon brings up the question, whether especially the combination of high dopant concentrations and multicrystalline silicon leads to scattering effects that are not taken into account in the established mobility models and therefore lead to a stronger reduction in mobility than predicted. Further measurements of the mobility in compensated mc silicon are currently performed to proof the difference between experiment and theory on a more statistical base.

5 CONCLUSIONS

In this contribution, we investigated the influence of compensation on the majority conductivity mobility and the Hall mobility in p-type multicrystalline silicon wafers. For the not compensated wafer good agreement with the mobility predicted by Klaassen was achieved, whereas the mobilities in the compensated umg-Si wafers are significantly lower than predicted by Klaassen's model. The difference between experiment and theory increases with increasing total dopant concentration. As there are mobility measurements on compensated monocrystalline silicon which show good agreement with Klaassen's model, further investigations should concentrate on the question, whether the difference between model and measurements reported here is due to scattering mechanisms in compensated multicrystalline silicon that are not accounted for in the established mobility models.

Further we determined the Hall factors, which vary from 0.75 to 0.84 and tend to increase with increasing dopant concentration.

ACKNOWLEDGEMENT

We thank Janina Posdziech for performing the Hall measurements and we acknowledge financial support by the German Federal Ministry for the Environment,

Nature Conservation and Nuclear Safety (Contract Number 0329988C) under the frame of the project "ALBA II" and the provision of multicrystalline wafers by QCells.

REFERENCES

[1] A. Cuevas and D. Macdonald, Silicon Forest, Falkau, Germany (2009).
[2] A.B. Sproul, M.A. Green, and A.W. Stephens, Journal of Applied Physics **72** (9), 4161 (1992).
[3] F.E. Rougieux, D. Macdonald, A. Cuevas, S. Ruffell, J. Schmidt, B. Lim, and A.P. Knights, Journal of Applied Physics **108**, 013706 (2010).
[4] D.K. Schroder, Semiconductor material and device characterisation (1990).
[5] J.F. Lin, S.S. Li, L.C. Linares, and K.W. Teng, Solid-State Electronics **24** (9), 827 (1981).
[6] F. Szmulowicz, Physical Review B, **24** (6), 4031 (1986).
[7] J. Geilker, W. Kwapil, I. Reis, S. Rein, Proceedings of the 25th EU PVSEC, Valencia, Spain, 2CO.2.6 (2010).
[8] R. Bock, P.P. Altermatt, and J. Schmidt, Proceedings of the 23rd EU PVSEC, Valencia, Spain, 1510 (2008).
[9] D. Macdonald, A. Cuevas, and L.J. Geerligs, Applied Physics Letters **92**, 202119 (2008).
[10] D.M. Caughey and R.E. Thomas, Proceedings of the IEEE **55** (12), 2192 (1967).
[11] D.B.M. Klaassen, Solid-State Electronics **35** (7), 953 (1992).
[12] J. Libal, S. Novaglia, M. Acciarri, S. Binetti, R. Petres, J. Arumughan, R. Kopecek, and A. Prokopenko, Journal of Applied Physics **104**, 104507 (2008).